Eur. Phys. J. B **40**, 209–215 (2004)
DOI: 10.1140/epjb/e2004-00259-9

THE EUROPEAN PHYSICAL JOURNAL B

Interaction between a BSCCO-type intrinsic Josephson junction and a microwave cavity

S. Madsen[1], G. Filatrella[2,a], and N.F. Pedersen[1]

[1] Oersted-DTU, Section of Electric Power Engineering, The Technical University of Denmark, 2800 Lyngby, Denmark
[2] INFM/Coherentia and Dept. of Biological and Environmental Sciences, University of Sannio, Via Port'Arsa 11, 82100 Benevento, Italy

Received 9 March 2004 / Received in final form 6 June 2004
Published online 12 August 2004 –

Abstract. The electrical behavior of anisotropic BSCCO single crystals is modeled by mutually coupled long Josephson junctions. We show that although the fluxons in the different layers do not a priori prefer the in-phase motion desired for many potential applications it is possible to induce such behavior by coupling the system to a high-Q resonator with a resonance frequency corresponding to fluxon in-phase motion. The resulting model is a set of coupled non-linear partial differential equations. By direct numerical simulations we have demonstrated that the qualitative behavior of the combined stacked long Josephson junctions and cavity system can be understood on the basis of the general concepts of nonlinear oscillators interacting with a resonator. For some region of the parameter space it is possible to reach the desired synchronous state, making the system potentially suitable for applications. We also look at the different dynamical states defined by different fluxon dynamical states in combination with different cavity properties.

PACS. 74.50.+r Tunneling phenomena; point contacts, weak links, Josephson effects – 05.45.Xt Synchronization; coupled oscillators – 85.25.Cp Josephson devices

1 Introduction

Fluxon motion in intrinsic Josephson junctions of the highly anisotropic BSCCO type [1] offers a potentially interesting system for microwave applications in the hundreds of gigahertz – or even terahertz range. The basic physical mechanism to be exploited is the emission of electromagnetic radiation by a Josephson fluxon when it hits an edge of the junction. If it were possible to achieve an ordered motion of the Josephson fluxons in the various layers, the fluxons would hit the sides of the junctions simultaneously and emit electromagnetic radiation coherently. The difficulty arises from the fact that same polarity fluxons basically repel each other and therefore this simple argument would rather favor anti-phase motion. Strong dynamic effects of the extremely nonlinear system, however, may have the opposite effect and induce the desired synchronous fluxon motion with a corresponding characteristic velocity/frequency. If we embed the BSCCO system in a cavity with a resonance frequency corresponding to the in-phase fluxon frequency we may impose frequency locking and forced motion on the fluxon system. This is a generic behavior and a well known effect for other non-linear oscillator – cavity systems; it has particularly been observed for small [2] and long [3–5] Josephson junctions. To theoretically treat this problem several approaches related to Josephson physics have been proposed: series array of small Josephson junctions have been analyzed through the Liapunov exponents to characterize the tendency to phase-lock [6]; two-dimensional arrays or parallel and series long Josephson junctions have been treated with a model similar to the generic Kuramoto model for nonlinear interacting oscillators [7–9]. In spite of the wide use of the idea the application to stacks requires some special care. In fact in series arrays the basic nonlinear elements (small or long Josephson junctions) are independent and coupled only via the resonator. The role of the cavity is to favor the in phase mode to prevent the junctions to wander around with arbitrary phase-shift. In such cases in the ideal situation of identical junctions the synchronous motion could be obtained if the coupling mechanism is able to provide any attraction – even arbitrarily small. For such reason the investigations of the previous systems focused on non-identical junctions – i.e. on oscillators whose natural frequency are different, to estimate the capability of the locking mechanism to overcome the differences due to fabrication imperfections in the junctions parameters [7,10,11]. For intrinsic junctions the crucial point, as already mentioned, is that even perfectly identical junctions would not oscillate in-phase. For such reason in this work we focus on identical junctions coupled to a

[a] e-mail: filatrella@unisannio.it

cavity. A preliminary study of the same system has been already presented elsewhere [12]; here we will present the mathematical model in Section 2, while in Section 3 we demonstrate numerical examples on the model for different situations with respect to the junction dynamical state and the cavity resonance frequency. As guidance to experimentalists searching for the practical applications we also calculate the emitted power and relate it to the junction dynamical states from which the radiation derives. Some conclusions are outlined in the last section.

2 The model

The standard model for inductively coupled stacks is a set of Partial Differential Equations (PDE) coupled via the magnetic flux [13]:

$$\mathbf{SJ} = \frac{\partial^2 \phi}{\partial x^2}; \quad \mathbf{S} \equiv \begin{pmatrix} 1 & S & & & \\ S & 1 & S & & 0 \\ & \cdot & \cdot & \cdot & \\ & & \cdot & \cdot & \cdot \\ & 0 & & S & 1 & S \\ & & & & S & 1 \end{pmatrix};$$

$$J_i \equiv \frac{\partial^2 \phi_i}{\partial t^2} + \alpha \frac{\partial \phi_i}{\partial t} + \sin(\phi_i) - \gamma. \quad (1)$$

Here $\alpha = (1/R_j)(\hbar/2eI_0C_j)^{1/2}$ is the dissipation parameter (R_j, I_0, and C_j are the normal resistance, the critical current and the capacitance per unit length, respectively), γ is the current normalized to the critical current I_0 of the individual junctions, is the normalized coupling term among the junctions in the stack reads $S = -\lambda_L/d' \sinh(t/\lambda_L)$, $d' = d + 2\lambda_L \coth(\tau/\lambda_L)$ [13]. Time is normalized to the inverse of the Josephson frequency $\omega_j = (2eI_0/\hbar C_j)^{1/2}$ and space with respect to the Josephson length $\lambda_j = (\hbar/2e\mu_0 I_0)^{1/2}$. The resonator at one edge of the junctions (see Fig. 1) changes the boundary conditions: instead of the open circuit conditions (or zero spatial derivatives) one should introduce a term proportional to the current fed by the resonator that causes a magnetic field which changes the boundary conditions [14]. The new boundary condition is:

$$\frac{\partial \phi_i}{\partial x} = \gamma_i. \quad (2)$$

Here $\gamma_i = I_i/I_0$ is the normalized current at the right hand side of the LJJ (see Fig. 1). Such current is connected to the normalized (respect to I_0/ω_j) charge q in the capacitor of the RLC circuit via the equation:

$$\gamma_i = -\frac{1}{N}\left(\frac{2a}{\Omega^2}\frac{d^2q}{dt^2} + \frac{1}{\Omega^2}\frac{d^3q}{dt^3}\right) + \frac{c}{N}\frac{\partial^2 \phi_i(L)}{\partial t^2}. \quad (3)$$

Here Ω is the resonance frequency of the RLC circuit normalized to the Josephson frequency ω_j, $\Omega = \sqrt{(1/(NC_0L))/\omega_j}$, Q its quality factor, $a = \Omega/2Q$ is the dissipation in the cavity, c is the total capacitance normalized to the Josephson capacitance, $c = NC_0/C_j$. The

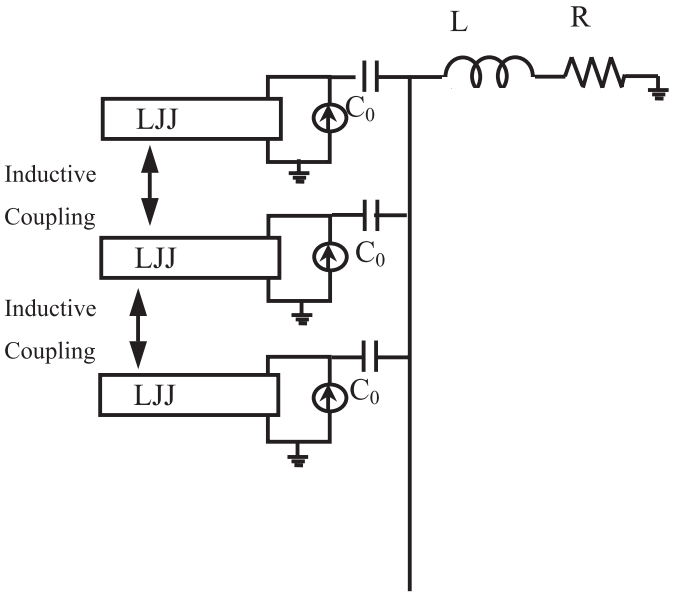

Fig. 1. Schematic drawing of the model.

charge in the resonator is given by the standard linear equation for the charge of a RLC circuit:

$$\frac{d^2q}{dt^2} + 2a\frac{dq}{dt} + \Omega^2 q = \Omega^2 \frac{c}{N}\sum_{i=1}^{N}\frac{\partial \phi_i(L)}{\partial t}. \quad (4)$$

Equations (1–4) have been integrated with a standard fourth (sometimes fifth) order Runge-Kutta routine for the time dependence. The spatial derivative has been approximated by the two-points discrete finite difference for the first derivative and the three-points finite difference for the second derivative.

The basic idea is that the fundamental oscillators (the fluxons moving back and forth in the individual junction layers) emit pulsed radiation at a frequency close to the resonance frequency of the cavity. At each collision some small amount of power – depending on the coupling coefficient – is transferred to the cavity. The current waveform in the (linear) cavity is essentially sinusoidal, and the amplitude builds up over many oscillation periods until a power balance is obtained, such that the power transferred to the cavity in each period is equivalent to the power transferred from the cavity to the junctions in the same period. When the frequency of the oscillators is close enough to the resonance of the cavity, the cavity oscillations become large enough to furnish the clock that forces the junction oscillators to phase-lock to the cavity resonance frequency. If the junction parameters are such that intrinsically the in-phase motion is favored at a frequency close to the cavity resonance frequency, the cavity – junction interaction will stabilize the fluxon in-phase motion and contribute even further to the build up of power in the cavity. In some cases with slightly different individual oscillation frequencies the above process becomes a cascade process with an abrupt transition from the unlocked to the locked state with a sudden increase in the degree of coherence [2,7].

We note as a general feature of our system that it is an unusual variant of the classical problem of a nonlinear oscillator coupled to a linear resonator. Here all the individual oscillators are each coupled to the cavity. In addition the individual oscillators are coupled to each other by inductive coupling, defining a number of different intrinsic oscillation modes. The competition between the two different types of coupling of the junctions will be essential for the outcome of the dynamics, and the possibilities for utilizing the combined system for applications.

3 Numerical results

To introduce the topic, Figure 2 shows some results for a Josephson stack without any coupling to a cavity. We have chosen the smallest reasonable stack, $n = 3$, and kept the length short, in order to find the essentials of the problem without needing too excessive calculations. In the following we will need the characteristic velocities for electromagnetic waves in the stack considered as a linear resonator. For an N-stack there are N characteristic velocities for the N different modes of propagation for linear modes. These velocities depend on the coupling parameter S, and the simple formula for calculating these velocities may be found for example in reference [13]. Here we will consider only the in-phase velocity $\mathbf{C}^+$ and the anti-phase velocity $\mathbf{C}^-$:

$$C^{+,-} = C^0 \frac{1}{\sqrt{1 \pm S}} \quad C^0 = \sqrt{\mu_0 d' C_j}. \tag{5}$$

Figure 2 shows the average voltage per junction, as well as the phase difference between the top/bottom and center junction. The main observations of Figure 2 are: For bias current increasing from below we notice that the voltage gets locked at the resonant step at $V = (2\pi/L)\mathbf{C}^- \sim 1.20$, while the phase angle between the top/bottom and center fluxon decreases from about π to about 1 at a bias of $\gamma = 0.32$, where the center junction expels the fluxon and switches to a finite voltage. Thus below $\gamma = 0.32$ we have the anti-phase mode with a velocity close to the characteristic velocity $\mathbf{C}^-$. At larger bias currents the in-phase mode becomes stable. We notice that the voltage for γ between about 0.35 and 0.6 is defined by the in-phase velocity $\mathbf{C}^+$ through $V = (\pi/L)\mathbf{C}^+ \sim 1.34$ while in the same bias range the phase angle is zero, i.e. the fluxons in the three layers move coherently. At a bias around $\gamma = 0.6$ the in-phase motion becomes unstable and the middle fluxon is expelled; top and bottom junctions are still on the fluxon resonant mode while the middle junctionis now biased at a finite voltage defined by the McCumber curve. By decreasing the bias from $\gamma = 0.9$ to low bias ($\gamma \approx 0.3$) the two-fluxon solution is preserved to such a low bias.

While Figure 2 shows the case of no coupling of the junctions in the stack to a cavity, the case of no coupling between junctions but coupling to a common cavity has been considered previously [2–4]. For this case the junction oscillators are still nonlinear and frequency locking to a cavity may be observed as discussed in references [2–4].

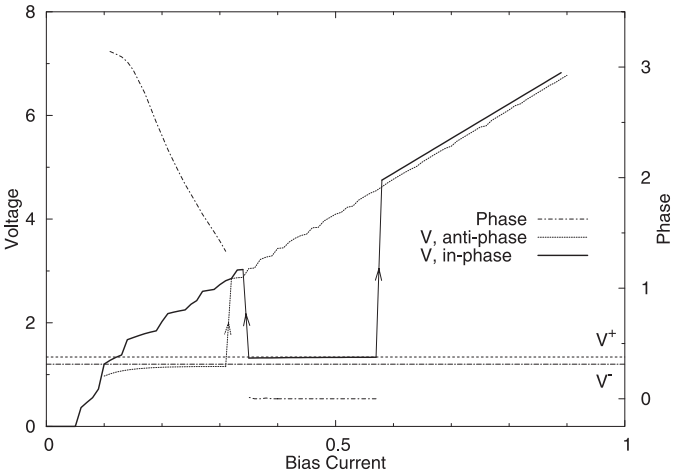

Fig. 2. Numerical example for a 3 junction stack without a cavity. Parameters of the simulations are: $n = 3$, $L = 5$, $\alpha = 0.05$, $S = 0.1$, $Q = 100$, $c = 0$. The two horizontal lines denotes the voltages corresponding to in-phase and anti-phase resonant steps, and the voltage is the average voltage per junction. The phase-difference of the solitons in the top and middle junction is also shown.

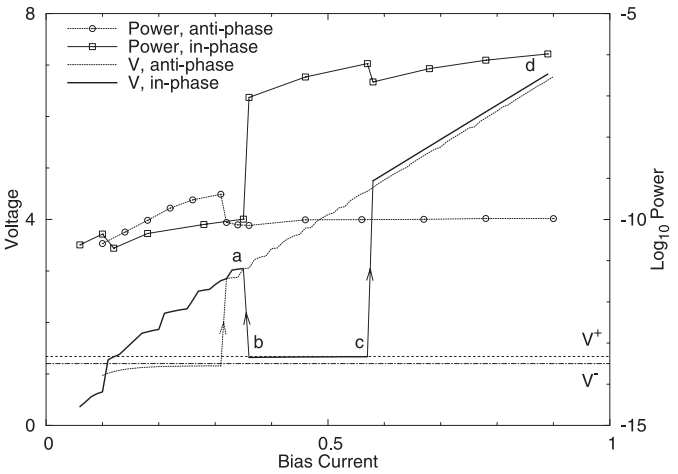

Fig. 3. Numerical example for a 3 junction stack with a cavity with resonant-frequency corresponding to the in-phase step. Parameters of the simulations are: $n = 3$, $L = 5$, $\alpha = 0.05$, $\varepsilon = 0.1$, $Q = 100$. $c = 0.001$, $\Omega = 0.67$. The two horizontal lines denotes the voltages corresponding to in-phase and anti-phase resonant steps, and the voltage is the average voltage per junction. Not shown is the phase-difference, because it is similar to the one plotted in Figure 2.

A cavity induced step may be observed in the IV curve, indicating frequency pulling of the junctions towards the cavity resonance frequency. Such a system may be obtained experimentally by fabricating several low T_c long Josephson junctions on the same substrate and putting them in a cavity.

In Figure 3 we have the combined effects of junction – junction coupling as well as junction – cavity coupling. Indeed Figure 3 shows some of the main results of this work. Like in Figure 2 we have chosen the smallest reasonable stack, $n = 3$, and kept the length short. This should

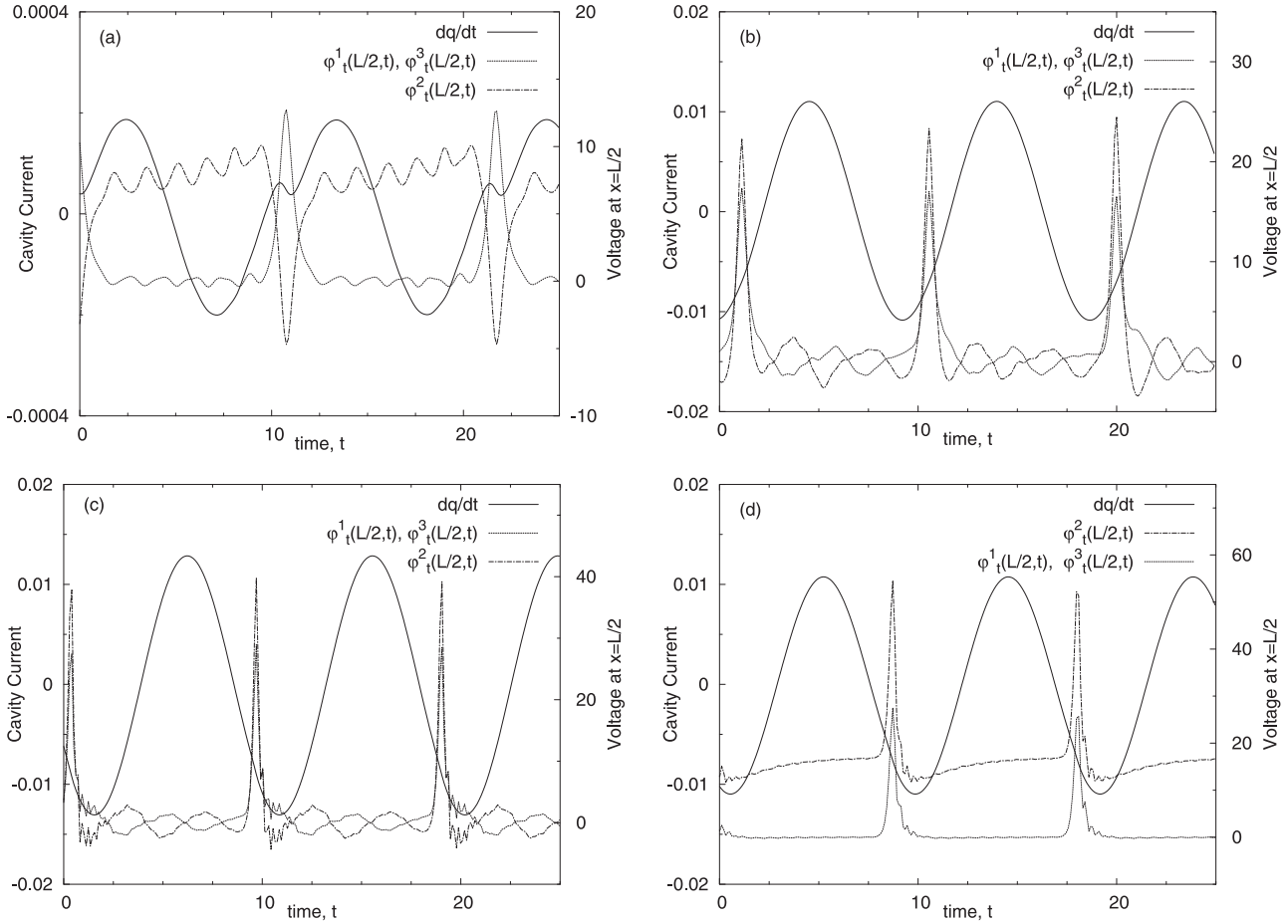

Fig. 4. Numerical examples for a 3 stack with a cavity. Parameters of the simulations are: $n = 3$, $L = 5$, $\alpha = 0.05$, $S = 0.1$, $Q = 100$, $c = 0.0001$, $\Omega = 0.67$. a) $\gamma = 0.34$, b) $\gamma = 0.35$, c) $\gamma = 0.56$, and d) $\gamma = 0.85$. The solid line denotes the current in the cavity (left axis) while the thick and thin dotted lines denote the middle and top/bottom junctions, respectively (right axis).

enable us to observe the essential phenomena while keeping the numerical work at a minimum. The figure shows the phase difference between the top/bottom fluxon and the center fluxon as a function of the bias current. We also show the average junction voltage (this is an experimentally observable quantity and a valuable tool to characterize the dynamical state. Finally we also show the (normalized) power, $P/I_0^2 L\omega_j$, in the cavity, calculated according to the formula equation (6):

$$\log_{10}\left(\frac{P}{LI_0\omega_j^2}\right) = \log_{10}\left\{\frac{\Omega}{Q}\frac{1}{T}\int_0^T \left(\frac{dq(t)}{dt}\right)^2 dt\right\}. \quad (6)$$

Here P is the average power dissipated in the resonator numerically retrieved through the current obtained from equation (4).

The three stack is loaded with a cavity in resonance with the in-phase mode defined in Figure 2, and we note that for a bias range between $\gamma = 0.34$ and $\gamma = 0.58$ the phase difference is zero and the voltage consistent in-phase motion through $V = (2\pi/L)\mathbf{C}^+ = 1.34$. Strictly speaking the in-phase voltage calculated this way may be slightly overestimated since small delays occur at the collisions with the boundaries. We find that this is a negligible effect here. Also we have chosen a rather small coupling coefficient of $S = 0.1$ while a typical value for BSCCO type material is larger, for example almost 0.5. We have calculated that case also, and find that the qualitative behavior we describe here is generic. We also note that the behavior in Figure 3 is not the only state: depending on the initial conditions other configurations are possible. However, if we compare to Figure 2, it seems clear that the cavity has increased the stability of the in-phase mode slightly for low bias. We notice that the power in the cavity decreases dramatically below $\gamma = 0.34$ and there is another transition to a slightly lower power at $\gamma = 0.58$. The origin of this may be understood from considering the more detailed time pictures shown in Figures 4a–d.

Figures 4a–d show the time behavior for selected bias points in Figure 3. In Figure 4a, the unperturbed motion of the fluxons in absenceof the resonator (which has resonance frequency $\Omega = 0.67$ corresponding to in-phase motion, compare to Fig. 2), for the lowest bias $\gamma = 0.34$ we would have had anti-phase fluxon motion. We note in Figure 4a that the center junction has expelled the fluxon and switched to the McCumber curve. The top and bottom junctions have each one fluxon, each fluxon in phase with the other. In fact while the top/bottom junctions

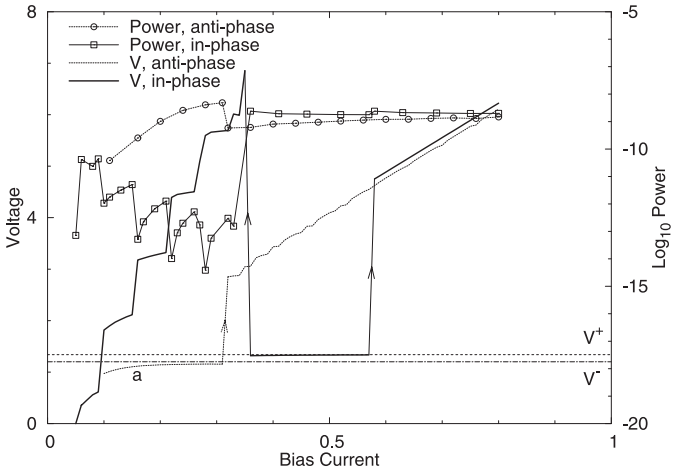

Fig. 5. Numerical example for a 3 junction stack with a cavity with resonant-frequency corresponding to the anti-phase step. Parameters of the simulations are: $n = 3$, $L = 5$, $\alpha = 0.05$, $S = 0.1$, $Q = 100$. $c = 0.0001$, $\Omega = 0.6$. The two horizontal lines denotes the voltages corresponding to in-phase and anti-phase resonant steps, and the voltage is the average voltage per junction. Not shown is the phase-difference, because it is similar to the one plotted in Figure 2.

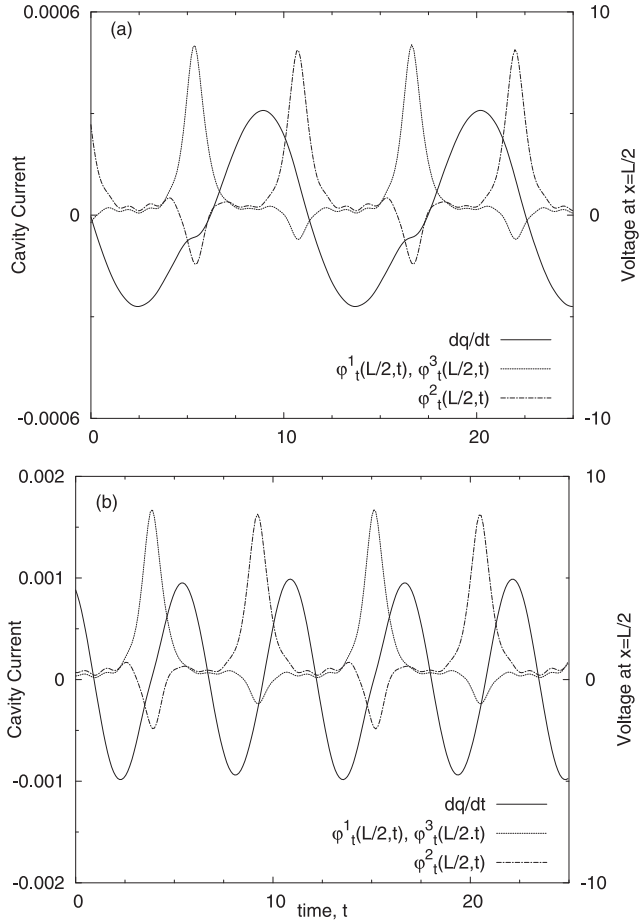

Fig. 6. Time pictures for a 3 stack with a cavity. Parameters of the simulations are: $n = 3$, $L = 5$, $\alpha = 0.05$, $S = 0.1$, $Q = 100$. $c = 0.0001$, $\gamma = 0.15$, $\Omega = 0.60$ (a) and $\Omega = 1.2$ (b). The solid line denotes the current in the cavity (left axis) while the thick and thin dotted lines denote the middle and top/bottom junctions, respectively (right axis).

voltages oscillate around the zero voltage value with a sudden peak corresponding to the fluxon passage, the middle junction shows a steady non-zero voltage corresponding to the uniform rotation of the phase. These fluxons induce a pulse (trace) with the opposite polarity on top of the finite voltage in the center junction. Thus when coupling to the cavity, the center junction pulse will subtract from the top/bottom fluxons and reduce the power in the cavity. This can be directly seen from the low value of the cavity current and from the decreased cavity power in Figure 3. In Figure 4b with a slightly increased bias, $\gamma = 0.35$ fluxons exist in all three junctions in an in-phase configuration moving with a velocity corresponding to C^+. This coherent motion is in resonance with the cavity, and gives rise to a cavity current 50 times larger than in Figure 4a. We note that the minimum of the cavity current is delayed about 45 degrees with respect to the arrival of the fluxons. At the upper range of stability of this mode, $\gamma = 0.56$ shown in Figure 4c, this phase angle is -45 degrees, while for $\gamma = 0.41$ (not shown) this phase angle is approximately zero. We also note in Figures 4b, c the small anti-phase oscillations which keep the fluxons locked in the in-phase mode. These oscillations are well known for stacked Josephson junctions [15–18]. In Figure 4d corresponding to $\gamma = 0.85$, a transition to still another mode has taken place. In this case, as in Figure 4a, the center junction has expelled its fluxon and switched to a finite voltage corresponding to the McCumber curve, as can be seen both from Figure 4d and Figure 3. In contrast to Figure 4a, the trace in the center junction is now in phase with the fluxons in the top/bottom junctions, and all three junctions contribute constructively to the cavity current which has almost the same value as for the in-phase fluxon mode in Figure 4c. Figure 3 also shows that the power in the cavity has only changed marginally. Our conclusion is that the microwave power generated does not change significantly if some junctions in the stack switch to the McCumber curve, as long as the trace has the same polarity as the fluxons. For a system without a cavity this was also pointed out in reference [19].

Figure 5 shows the case of the 3 – stack loaded with a cavity with a resonance frequency $\Omega = 0.60$ corresponding to the anti-phase motion. Several features in Figure 5 are similar to the decoupled system in Figure 2. For low values of the bias – γ smaller than about 0.30 – anti-phase motion with a decreasing phase difference is observed together with another mode in which all junctions have switched to the McCumber curve. The main difference is that, as it is evident from the slope of the I-V curve, in Figure 1 only one junction has switched to the McCumber. The power in the cavity is increasing with γ although it is several orders of magnitude smaller than for the in-phase situation in Figures 3, 4.

A time picture for low bias $\gamma = 0.15$ is shown in Figure 6a. We note that same polarity fluxons exist in all three junctions, however the center fluxon is

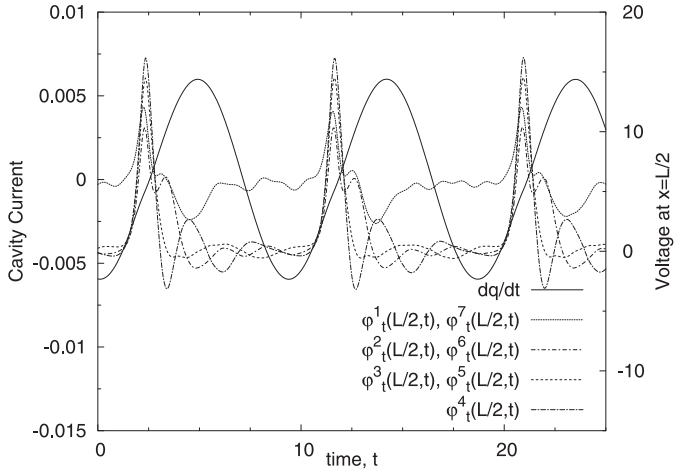

Fig. 7. Numerical example of a time picture for a 7 stack with an in-phase cavity. Parameters of the simulations are: $n = 7$, $L = 10$, $\alpha = 0.05$, $S = 0.1$ $Q = 100$, $c = 0.00233$, $\Omega = 0.3479$, $\gamma = 0.57$. The solid line denotes the current in the cavity (left axis) while the dotted lines denote the junction voltages (right axis).

approximately 180 degrees out of phase with the top/bottom fluxons as it should be for the anti-phase mode. All three fluxons leave traces with opposite polarity in neighboring junctions thus reducing the current coupled into the cavity. We also note that because of the anti-phase motion the fundamental frequency exiting the cavity is at twice the cavity resonance frequency. Hence the current and power in the cavity is small as can be seen from Figure 6a. When the stability range of the mode in Figure 6a is exceeded at $\gamma = 0.15$ the center junction switches while the top/bottom fluxons continue to move in-phase. They leave a trace in the center junction which has opposite polarity of the fluxons. The time picture looks much like in Figure 4a, and the power is small as can be seen from Figure 6a. Taking the consequences of the discussion in connection with Figure 6a we tried to load the junction with a cavity having a resonance frequency at twice the frequency corresponding to anti-phase motion, i.e. $\Omega = 1.20$, while leaving all other parameters unchanged. The result is shown in Figure 6b. Now we see essentially the same fluxon behavior as in Figure 6a; however the cavity current, now at the double frequency, becomes 3−4 times larger and hence the power in the cavity increases more than an order of magnitude. As the bias is increased towards the end of the stability range for this mode ($\gamma = 0.31$) the phase angle between the top/bottom and center junctions becomes smaller, as can be seen from Figure 6a, and the difference between cavities at the fundamental and second harmonic becomes less pronounced.

After having studied above the general behavior of the stacked junction – cavity system for the relatively simple case of three junctions with length 5, we consider in Figure 7 numerically much more demanding case of $n = 7$ and $L = 10$. Using the general formula for $\mathbf{C}^+$ [13] we find $\mathbf{C}^+ = 1.1075$, and with $L = 10$ we find the inphase cavity frequency to be $\Omega = 0.3479$ and the cavity locking voltage $V = (2\pi/L)\mathbf{C}^+ = 0.6958$. In order to keep the coupling of the individual junction to the cavity the same as above we have changed the c-value from $c = 0.0001$ to $c = 0.001 * 7/3 = 0.000233$. From [18] we have selected parameters corresponding to almost coherent fluxon motion in a 7-stack. In that mode the inner 5 junctions has in-phase fluxon motion while the top and bottom junctions have switched to the McCumber curve. For these two junctions there are traces with the same polarity and in-phase with the inner fluxons. The time picture is shown in Figure 7 that also demonstrates that we can excite a cavity current the same way as in Figures 3, 4 for the 3 stack system.

4 Conclusion

The system consisting of a stack of Josephson junctions coupled to a cavity has been investigated. We find that if the resonator has a resonance frequency corresponding to the in-phase intrinsic resonance of the stack [see Eq. (5)], large amounts of power can be coupled to the cavity. We have also found the coexistence of several dynamic states, to which correspond different levels of emitted power. A remarkable difference with the small Josephson junctions arrays considered in reference [2] is that the resonant velocity of modes pertaining to different number of locked solutions are different [13], in contrast with the simpler situation depicted in reference [2]. In the latter case it is possible to independently change the number of active oscillators and their frequency, thus making a detailed study of the sole effect of the number of active junctions simpler.

The system has a potential for practical applications in microwave generation using high T_c BSCCO single crystals at hundreds of Gigahertz.

Support from the ESF vortex program, the NATO science for Peace program and the Danish STVF program 'New superconductors' are acknowledged.

References

1. M. Tachiki, T. Yamashita, *Intrinsic Josephson effect and plasma oscillations in high T_c superconductors* (Elsevier, Amsterdam, 2001)
2. P. Barbara, A.B. Cawthorne, S.V. Shitov, C.J. Lobb, Phys. Rev. Lett. **82**, 1963 (1999)
3. S. Pagano, R. Monaco, G. Costabile IEEE Trans. Magn. **25**, 1080 (1989)
4. N. Grønbech-Jensen, R.D. Parmentier, N.F. Pedersen, Phys. Lett. A **142**, 427 (1989)
5. G. Filatrella, G. Rotoli, N. Grønbech-Jensen, R.D. Parmentier, N.F. Pedersen, J. Appl. Phys. **72**, 3179 (1992)
6. P. Hadley, M.R. Beasley, K. Wiesenfeld, Phys. Rev. B **38**, 8712 (1988); M. Dhamala, K. Wiesenfeld, Phys. Lett. A **292**, 269 (2002)

7. G. Filatrella, N.F. Pedersen, K. Wiesenfeld, Phys. Rev. E **61**, 2513 (2000); G. Filatrella, N.F. Pedersen, K. Wiesenfeld, IEEE Trans. Appl. Sup. **11**, 1184 (2001)
8. P. Barbara, G. Filatrella, C.J. Lobb, N.F. Pedersen, *Studies of High temperature superconductors - Studies of Josephson junction arrays (II)*, edited by A.V. Narlikar (NOVA publishers, 2002, ISBN:1-59033-204-0), Chap. 4
9. G. Filatrella, N.F. Pedersen, C.J. Lobb, P. Barbara, Eur. Phys. J. B **34**, 3 (2003)
10. K. Wiesenfeld, P. Colet, S. Strogatz, Phys. Rev. Lett. **76**, 404 (1996); K. Wiesenfeld, P. Colet, S. Strogatz, Phys. Rev. E **57**, 1563 (1998)
11. E. Almaas, D. Stroud, Phys. Rev. B **65**, 134502 (2002); E. Almaas, D. Stroud, Phys. Rev. B **67**, 064511 (2003)
12. N.F. Pedersen, G. Filatrella, Physica C, in print *(Proceedings of the M2S-HTSC conference, Rio de Janeiro, May 2003)*
13. S. Sakai, P. Bodin, N.F. Pedersen, J. Appl. Phys. **73**, 2411 (1993)
14. J.C. Eilbeck, P.S. Lomdahl, O.H. Olsen, M.R. Samuelsen, J. Appl. Phys. **57**, 861 (1985)
15. E. Goldobin, B.A. Malomed, A.V. Ustinov, Phys. Lett. A **266**, 67 (2000)
16. E. Goldobin, A. Walraff, N. Thyssen, A.V. Ustinov, Phys. Rev. B **57**, 130 (1998)
17. C. Gorria, P.L. Christiansen, Yu. B. Gaididei, V. Muto, N.F. Pedersen, M.P. Soerensen, Phys. Rev. B **68**, 035415 (2003)
18. S. Madsen, N.F. Pedersen, Phys. Rev. B **69**, 064507 (2004)
19. N.F. Pedersen, S. Madsen, Supercond. Sci. Technol. **17**, S117 (2004)